Supporting Information

Aligned Silicon Nanofins via the Directed Self-Assembly of PS-*b*-P4VP Block Copolymer and Metal Oxide Enhanced Pattern Transfer

Cian Cummins,[*a] Anushka Gangnaik,[b] Roisin A. Kelly,[b] Dipu Borah,[a,c] John O'Connell,[b] Nikolay Petkov,[b] Yordan M. Georgiev,[b] Justin D. Holmes[b,c] and Michael A. Morris[*a,c]

[a] Materials Research Group, Department of Chemistry and Tyndall National Institute, University College Cork, Cork, Ireland.
* E-mail: m.morris@ucc.ie, cian.a.cummins@gmail.com
[b] Materials Chemistry and Analysis Group, Department of Chemistry and Tyndall National Institute, University College Cork, Cork, Ireland.
[c] Centre for Research on Adaptive Nanostructures and Nanodevices (CRANN/AMBER), Trinity College Dublin, Dublin, Ireland.

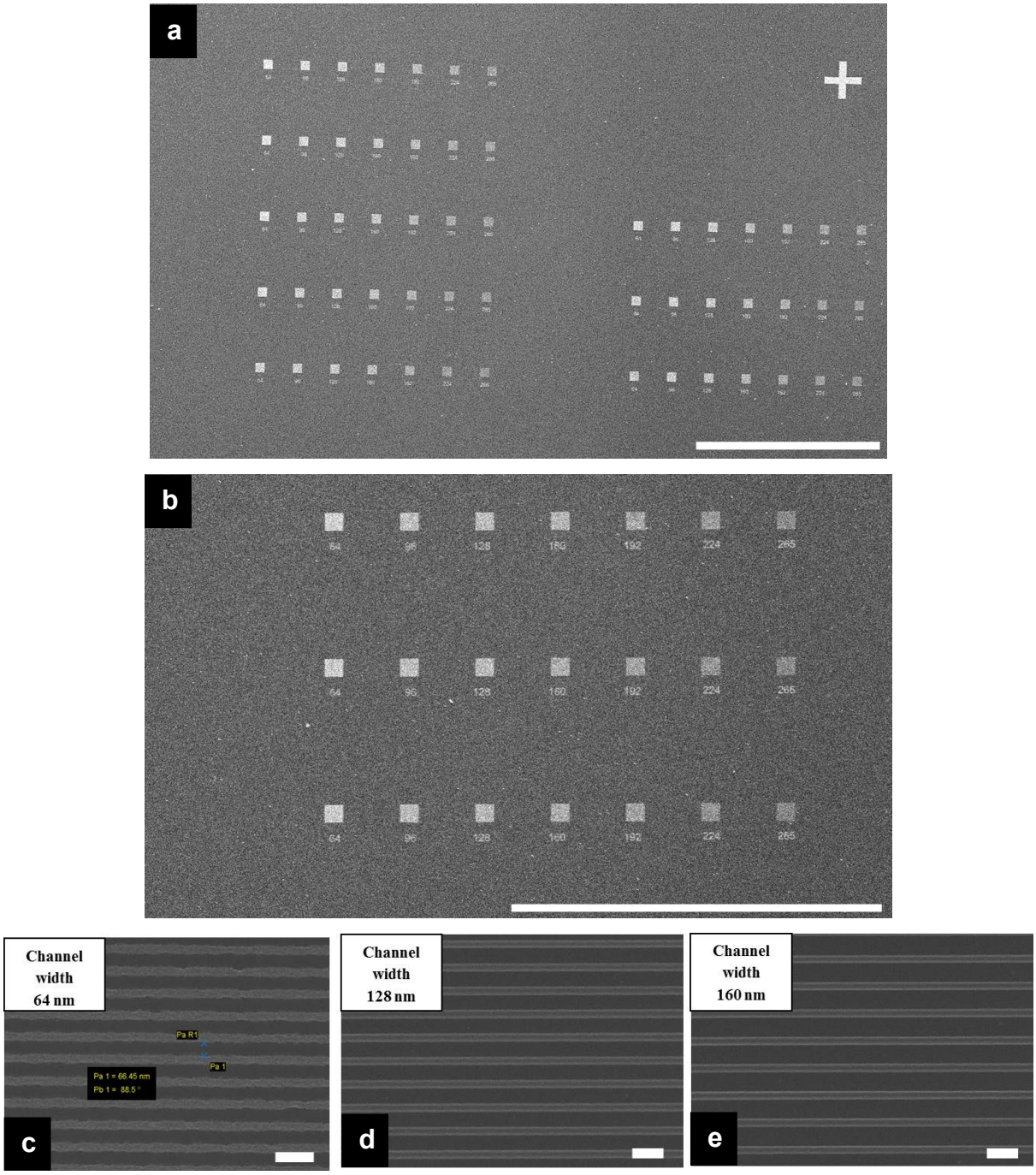

Figure S1. (a) and (b) (scale bars = 500 μm) show top-down SEM images of HSQ arrays following preparation as outlined in the experimental section in manuscript. High resolution top-down SEM images are shown in (c)-(e) (scale bars = 200 nm) of the HSQ trenches with channel widths of 64 nm, 128 nm and 160 nm respectively.

From our study of the thicker PS-*b*-P4VP films below (1 wt % and 2 wt %) it can be seen that P4VP C_{II} (*i.e.* parallel cylinders) can also be developed during some periods (*e.g.* Figure S3). However, the quality of the features is extremely poor in comparison to the 0.5 wt % films. Notably, 'relief' features associated with thicker films create non-uniform films increasing defect features.

It is evident that this PS-*b*-P4VP system forms C_{II} due to the film thickness, balanced interfacial interactions and the solvent vapor anneal (SVA) conditions. With these contributing issues evaluated, 0.5 wt % PS-*b*-P4VP films were deposited on substrates ultrasonically cleaned with organic solvent. Additionally, 0.5 wt % films SVA with chloroform for 2 – 4 hours were used that possessed long correlation lengths.

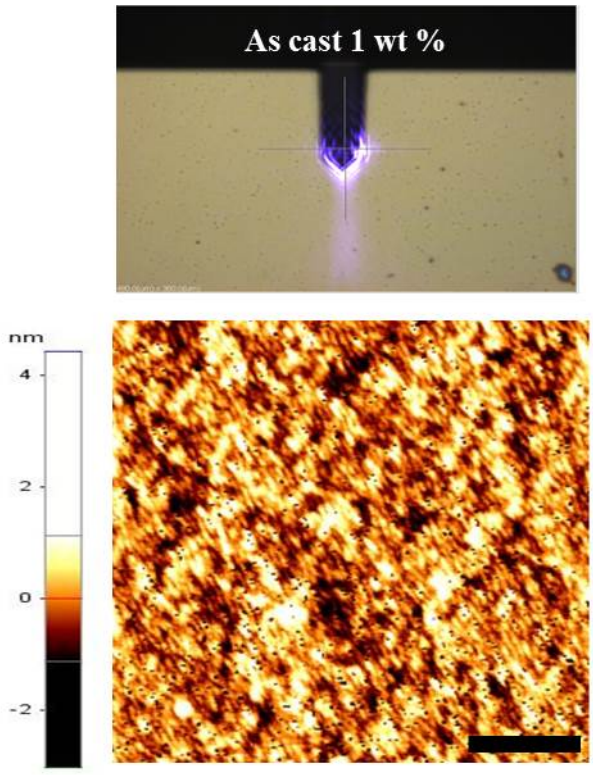

Figure S2. Optical image (~ 480 x 360 micron) (top) shows a uniform film following spin coating of 1 wt % PS-*b*-P4VP BCP thin film on an acetone cleaned silicon substrate. AFM topographic image (bottom, scale bar = 400 nm) reveals a poorly microphase separated structure. There appears to be some microphase separated features but these are not distinct.

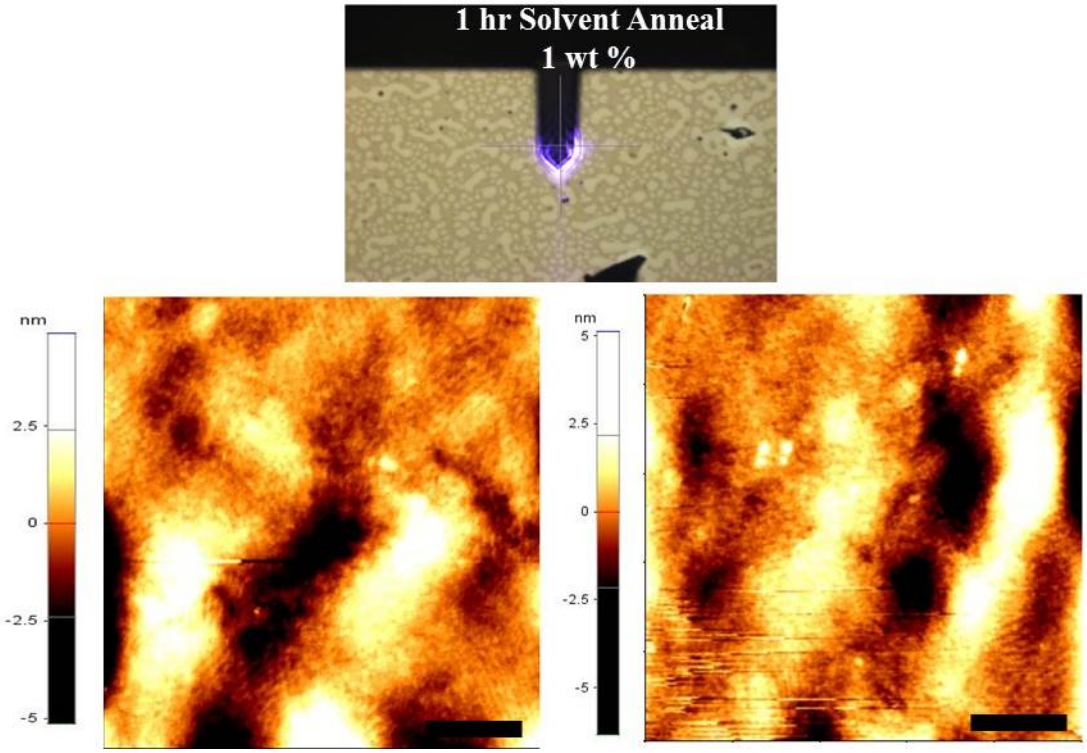

Figure S3. Optical image (top) (~ 480 x 360 micron) show areas of 1 wt % PS-*b*-P4VP BCP film with dewetting present after 1 hour solvent vapor annealing with chloroform. The AFM topographic image (bottom left, scale bar = 400 nm) is from a bright area in the optical image. The image shows formation of P4VP C_{II}, *i.e.* parallel to the substrate surface. Likewise the AFM topographic image (bottom right, scale bar = 400 nm) from the dark areas of the films shows P4VP C_{II}. We do not observe C_{II} across the whole film due to its non-uniformity. This is evident in both AFM images.

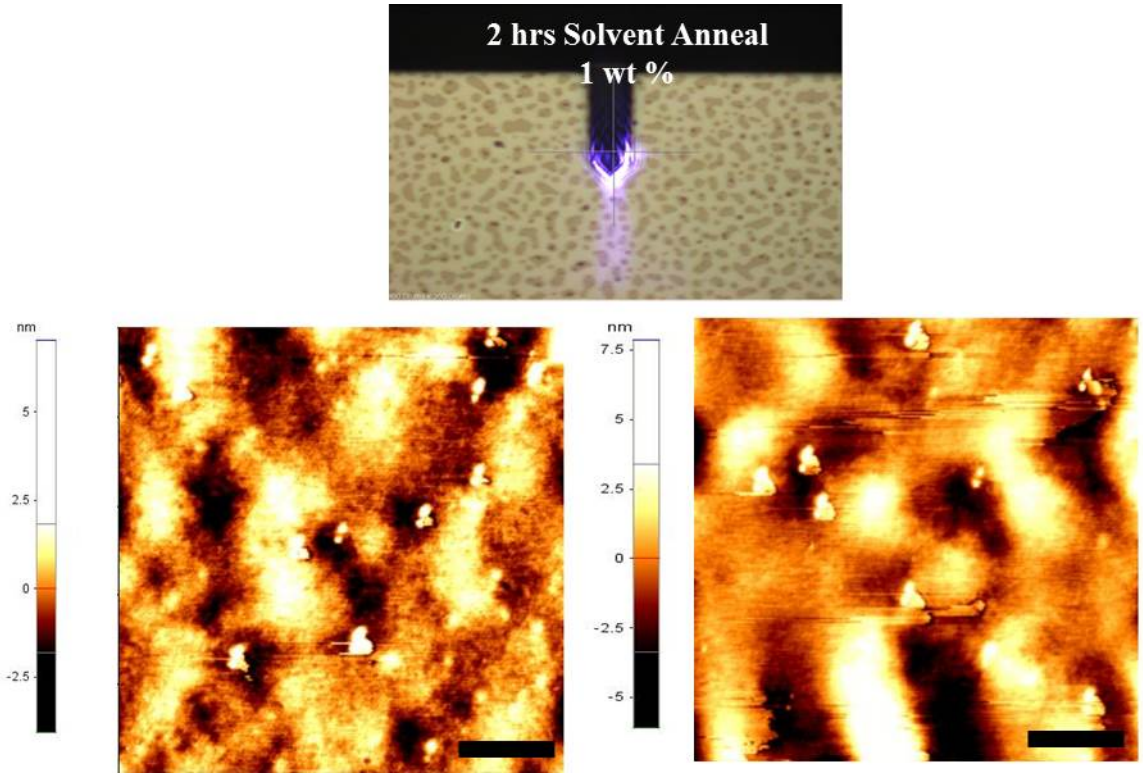

Figure S4. After 2 hours solvent vapor annealing the 1 wt % PS-*b*-P4VP BCP film, the optical image (top) (~ 480 x 360 micron) shows that the bright regions have grown from 1 hour solvent vapor annealing. The AFM topographic image (bottom left, scale bar = 400 nm) does not show any microphase separation. Likewise the AFM topographic image (bottom right, scale bar = 400 nm) does not show any hexgonal patterns. The height scale bars of both images show a non-uniform film surface with regions differing by at least 10 nm.

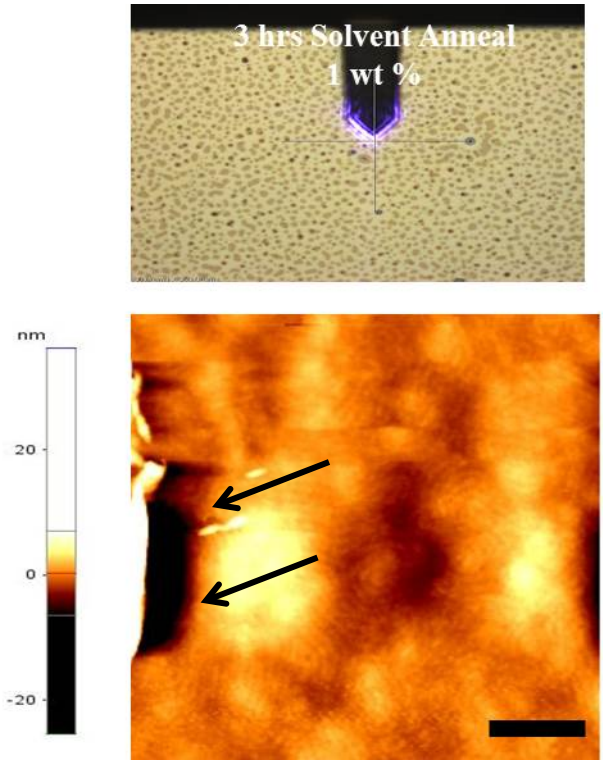

Figure S5. After 3 hours solvent vapor annealing the 1 wt % PS-*b*-P4VP BCP film, optical image (top) (~ 480 x 360 micron) reveals a greater coverage of the bright regions compared to the optical image in Figure S4. The AFM topographic image (bottom, scale bar = 400 nm) shows areas of microphase separated patterns (C_{II}), however these areas are not distinct due to the non-unifrom nature of the film. Areas of dewetting are also evident in the AFM image with greater that 20 nm depth (area indicated by arrows).

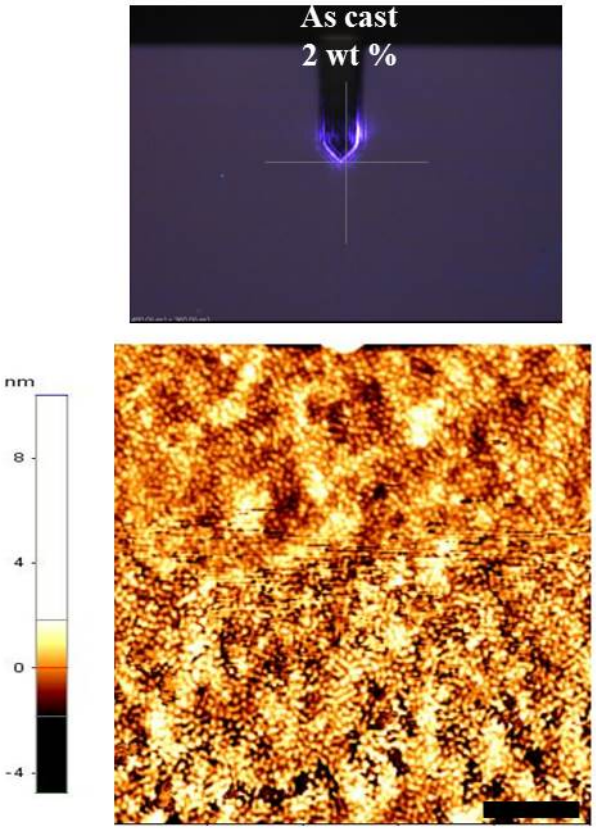

Figure S6. As cast optical image (top) (~ 480 x 360 micron) of the PS-*b*-P4VP BCP film following spin coating from a 2 wt % PS-*b*-P4VP solution on an acetone cleaned silicon substrate. AFM topogrpahic image (bottom, scale bar = 400 nm) shows microphase separated structures. The film shows cylinders normal to the substrate, however these have extremely poor order. These films have a distinct purple color.

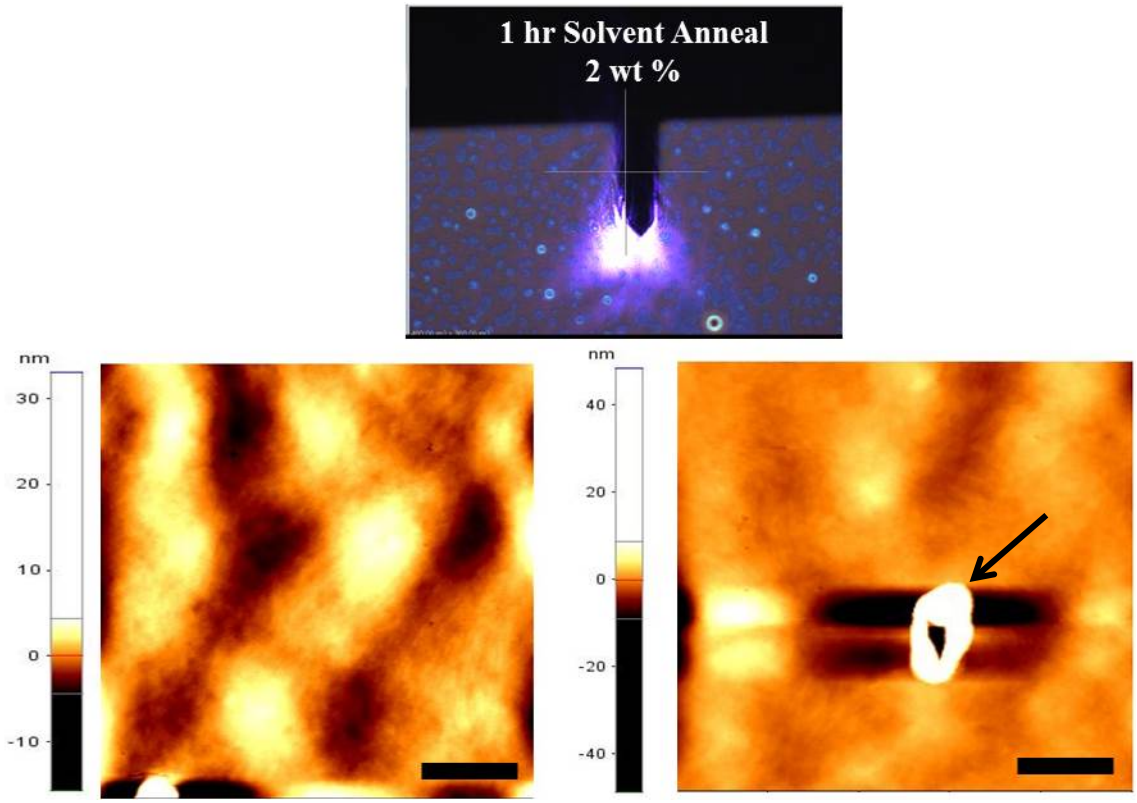

Figure S7. Optical image (top) (~ 480 x 360 micron) reveals a non-uniform film following 1 hour of solvent vapor annealing with chloroform from a 2 wt % PS-*b*-P4VP BCP film. The AFM topographic image of the blue area of optical image (bottom left, scale bar = 400 nm) shows a featureless surface with height variation as seen from the height to the left of the image. Also the brown area (AFM image, bottom right, scale bar = 400 nm) reveals a similar topography. The feature in the centre of the image (indicated by arrow) shows a height difference of more than 40 nm.

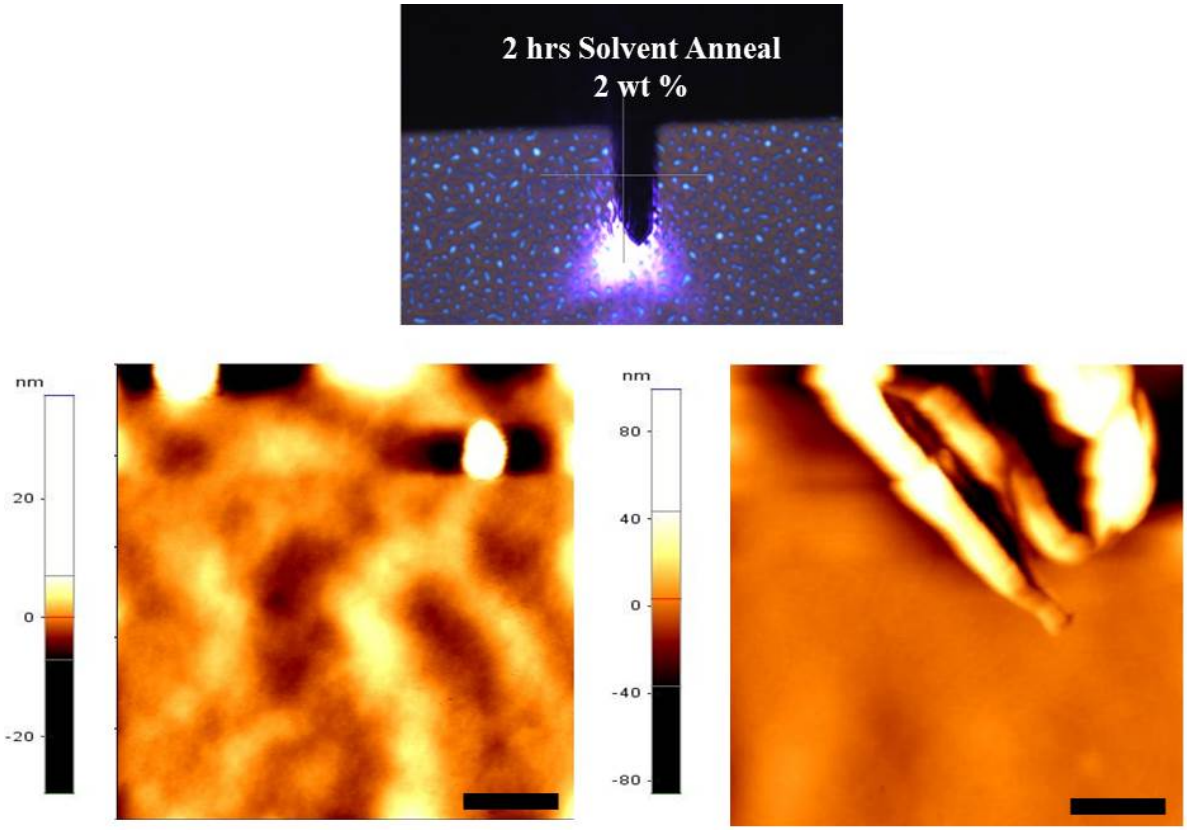

Figure 8. The optical image (top) (~ 480 x 360 micron) shows film surface following 2 hours of solvent vapor annealing with chloroform from a 2 wt % PS-*b*-P4VP BCP film. Both AFM topographic images (scale bars = 400 nm) do not show any microphase separated areas. Blue areas (bottom left) and brown areas (bottom right) scanned show relief structures with greater than 50 nm depth in some areas. The film thickness not being an integer of the periodicty of the nanodomain results in such formations.

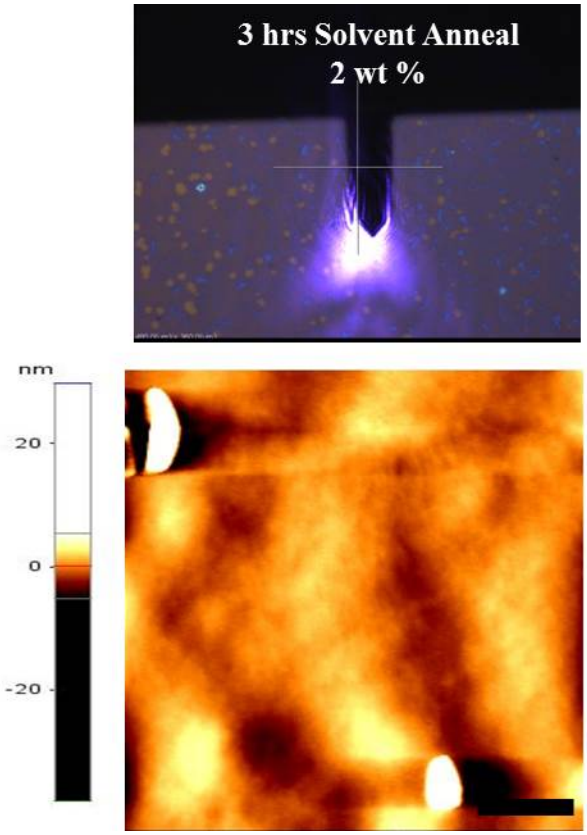

Figure S9. The AFM topographic image (bottom, scale bar = 400 nm) shows featureless areas following 3 hours of solvent vapor annealing with chloroform from a 2 wt % PS-*b*-P4VP BCP film. Microphase separation was absent from the film.

A screening procedure was also carried out with regard to different surface chemistries for the 0.5 wt % PS-*b*-P4VP films and only chloroform was used for SVA at ambient conditions. The contact angles were measured for all modified silicon substrate surfaces (see Figure S10). Surface chemistries analysed included ultraviolet/ozone (UV/O_3) cleaned, piranha cleaned, acetone cleaned, bare Si without any cleaning, PS-OH functionalized and PDMS-OH functionalized silicon. It was found that P4VP $C_{\perp}$ to the substrate were formed following spin coating on all surface chemistries studied except for PDMS-OH functionalized silicon surfaces (see Figure S16c). Although a piranha cleaned silicon surface showed P4VP C_{II} after SVA (see Figure S12d), areas of dewetting are present suggesting that the silicon surface is too hydrophilic and thus the hydrophilic PVP block interaction with the surface causes instability in the thin film. Likewise, the use of a hydrophobic (PDMS-OH functionalized) silicon surface did not exhibit any microphase separation for spin cast or solvent vapor annealed films (See Figure S16 c and d).

Methods and materials for silicon substrate surface chemistry modifications:

UV/ozone: Substrates were placed in UV/ozone system (PSD Pro Series Digital UV Ozone System; Novascan Technologies, Inc., USA) for a 30 minute treatment period.

Piranha cleaned substrates: Substrates were placed in a 'piranha' bath (sulfuric acid:hydrogen peroxide, 3:1) for 1 hour at 100°C. After piranha cleaning, substrates were cleaned and washed repeatedly with DI water. They were then blown dry under N_2 flow.

Acetone: As described in the manuscript, substrates were sonicated in acetone for 20 minutes and blown dry under N_2 flow.

Bare Si: Substrates were used as received and no cleaning or modification was employed.

PS-OH functionalized Si: Hydroxyl terminated polystyrene (PS-OH) was purchased from Polymer Source, Inc., Canada. The material's total number average molecular weight M_n= 6 kg mol^{-1} and has a polydisperity of 1.05 and was not further modified. 1 wt % solutions of PS-OH (6k) were made up in toluene and stirred for 1 hour until fully dissolved. 'Piranha' cleaned substrates were coated with the 1 wt % PS-OH (6k) solution at 3000 rpm and thermally annealed at 180°C for 6 hours. After annealing, the PS-OH modified films were then rinsed with toluene to remove any ungrafted PS-OH fragments.

PDMS-OH functionalized Si: Hydroxyl terminated polydimethylsiloxane (PDMS-OH) was purchased from Polymer Source, Inc., Canada. The material's total number average molecular weight M_n= 5 kg mol^{-1} and has a polydisperity of 1.07 and was not further modified. 1 wt % solutions of PDMS-OH (5k) were made up in toluene and stirred for 1 hour until fully dissolved. 'Piranha' cleaned substrates were coated with the 1 wt % PDMS-OH (6k) solution at 3000 rpm and thermally annealed at 180°C for 6 hours. After annealing, the PDMS-OH modified films were rinsed with toluene to remove any ungrafted PDMS-OH material.

All of the above modified surfaces were coated with a 0.5 wt % PS-*b*-P4VP BCP film and solvent vapor annealed with $CHCl_3$ vapor at room temperature (*i.e.*, in the manner described in the manuscript).

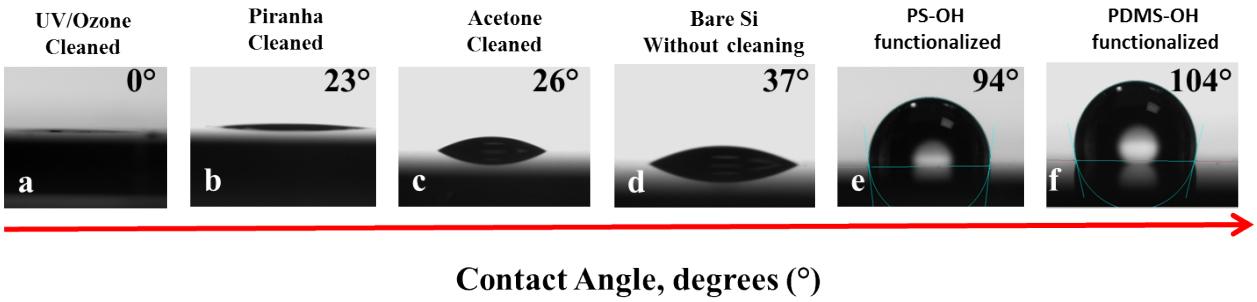

Figure S10. Contact angle (°) images of water droplets on (a) UV/ozone treated cleaned silicon (0°), (b) piranha cleaned silicon (23°), (c) acetone only cleaned silicon (26°), (d) bare silicon without cleaning (37°), (e) PS-OH functionalized silicon (94°) and (f) PDMS-OH functionalized silicon (104°).

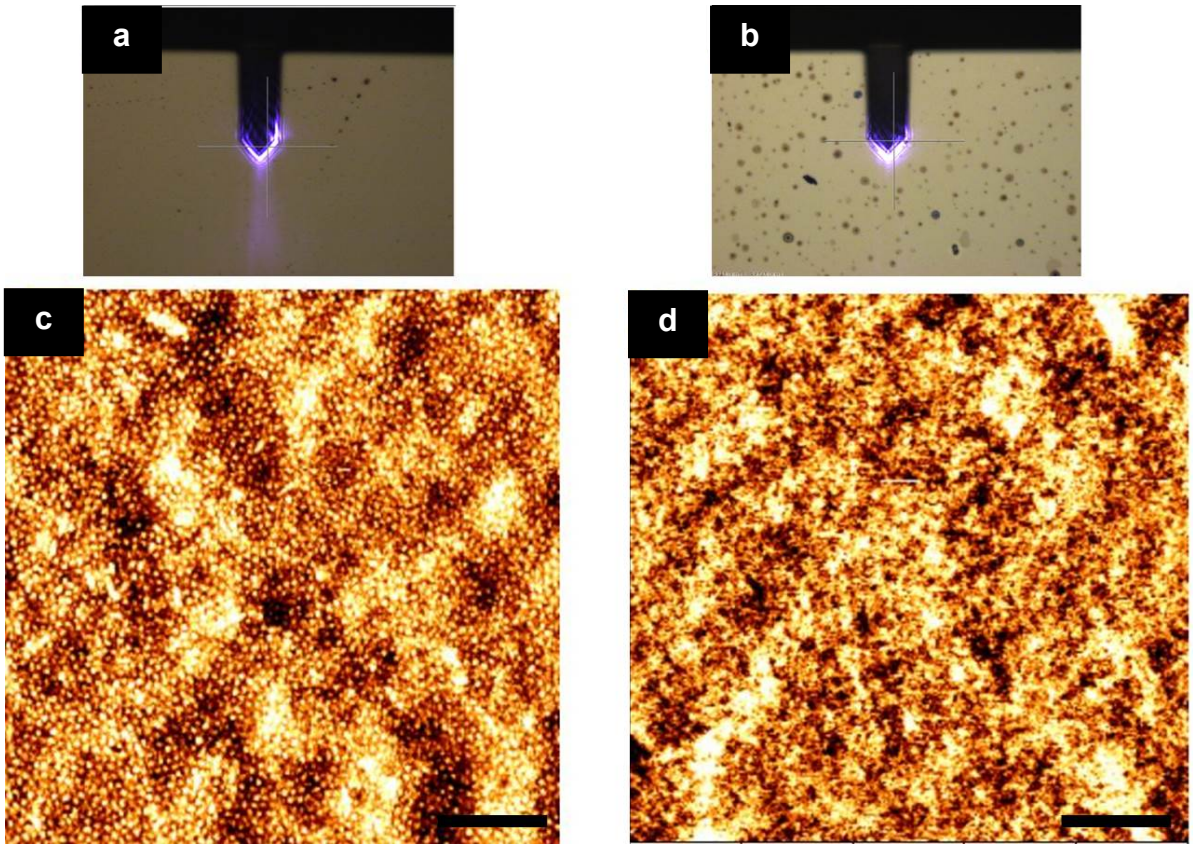

Figure S11. Optical images (~ 480 x 360 micron) of (a) as cast 0.5 wt % PS-*b*-P4VP on UV/ozone cleaned silicon sample (contact angle, 0°) and (b) following 2 hours of solvent vapor annealing with chloroform. Corresponding AFM topographic images (scale bar = 400 nm) are shown in (c) and (d). (c) AFM topographic image of as cast film showing poorly

ordered P4VP $C_{\perp}$ (normal) to the silicon substrate. (d) Following 2 hours solvent vapor annealing, the film is featureless.

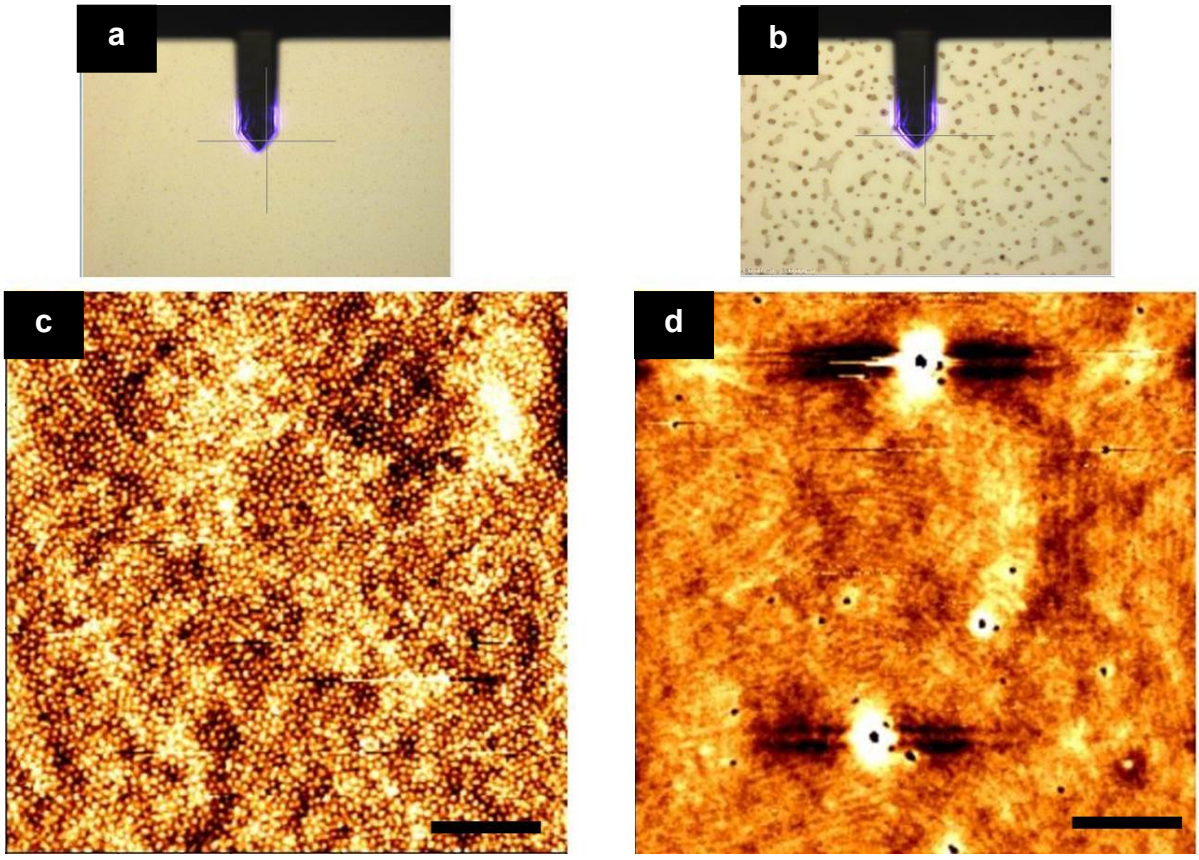

Figure S12. Optical images (~ 480 x 360 micron) of (a) as cast 0.5 wt % PS-*b*-P4VP on piranha cleaned silicon sample (contact angle, 23°) and (b) following 2 hours of solvent vapor annealing with chloroform. Corresponding AFM topographic images (scale bar = 400 nm) are shown in (c) and (d). (c) AFM topographic image of as cast film showing P4VP cylinders normal to the silicon substrate. (d) Following 2 hours solvent vapor annealing, the film shows P4VP cylinders lying in plane. Areas of dewetting can be seen in (d).

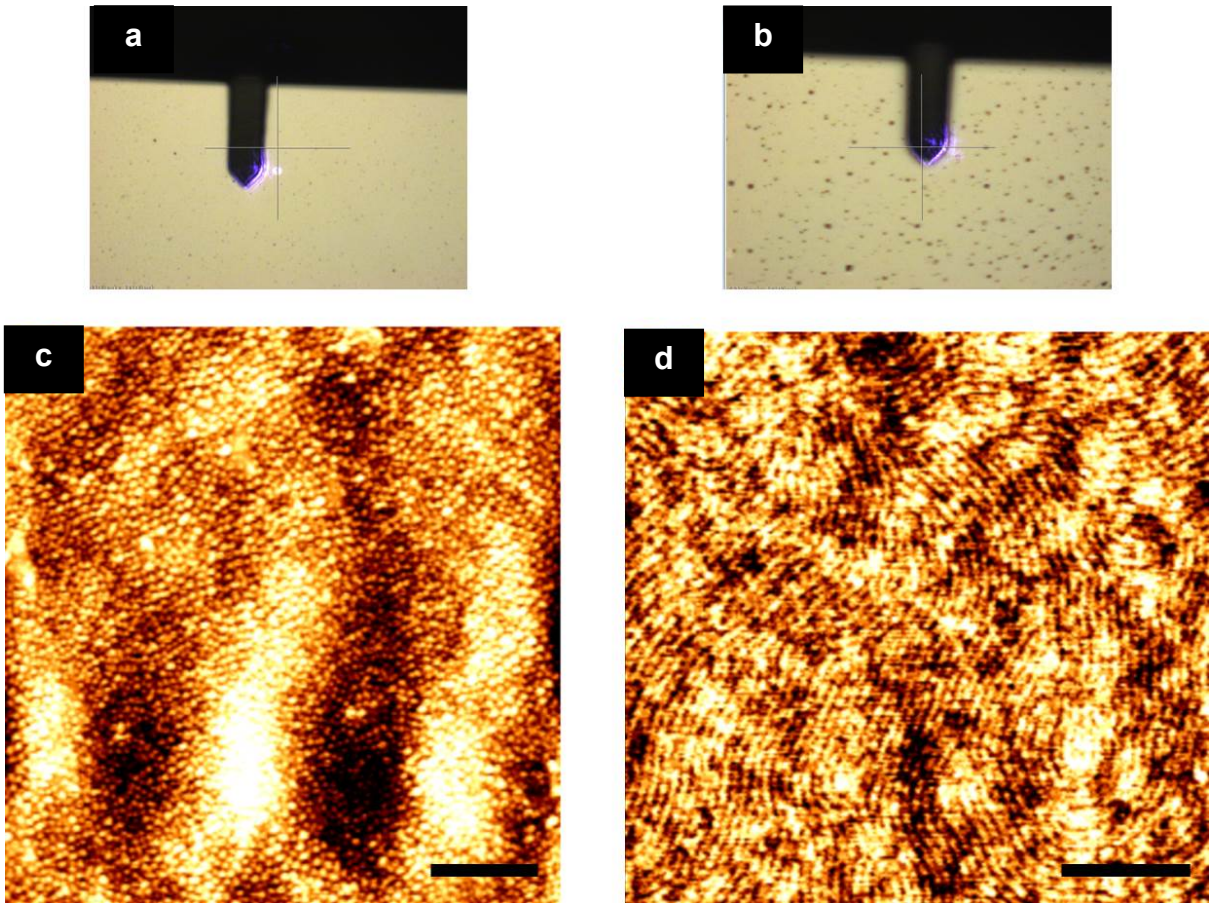

Figure S13. Optical images (~480 x 360 micron) of (a) as cast 0.5 wt % PS-*b*-P4VP on acetone only cleaned silicon sample (contact angle, 26°) and (b) following 2 hours of solvent vapor annealing with chloroform. Corresponding AFM topographic image (scale bar = 400 nm) of (a) is shown in (c). (c) AFM topographic image of as cast film showing P4VP cylinders normal to the silicon substrate. Corresponding AFM topographic image of (b) is shown in (d). A fully microphase separated pattern is observed with cylinder lying in plane. Reconstructed image in Figure 1 (c) in manuscript corresponds to Figure S13(d).

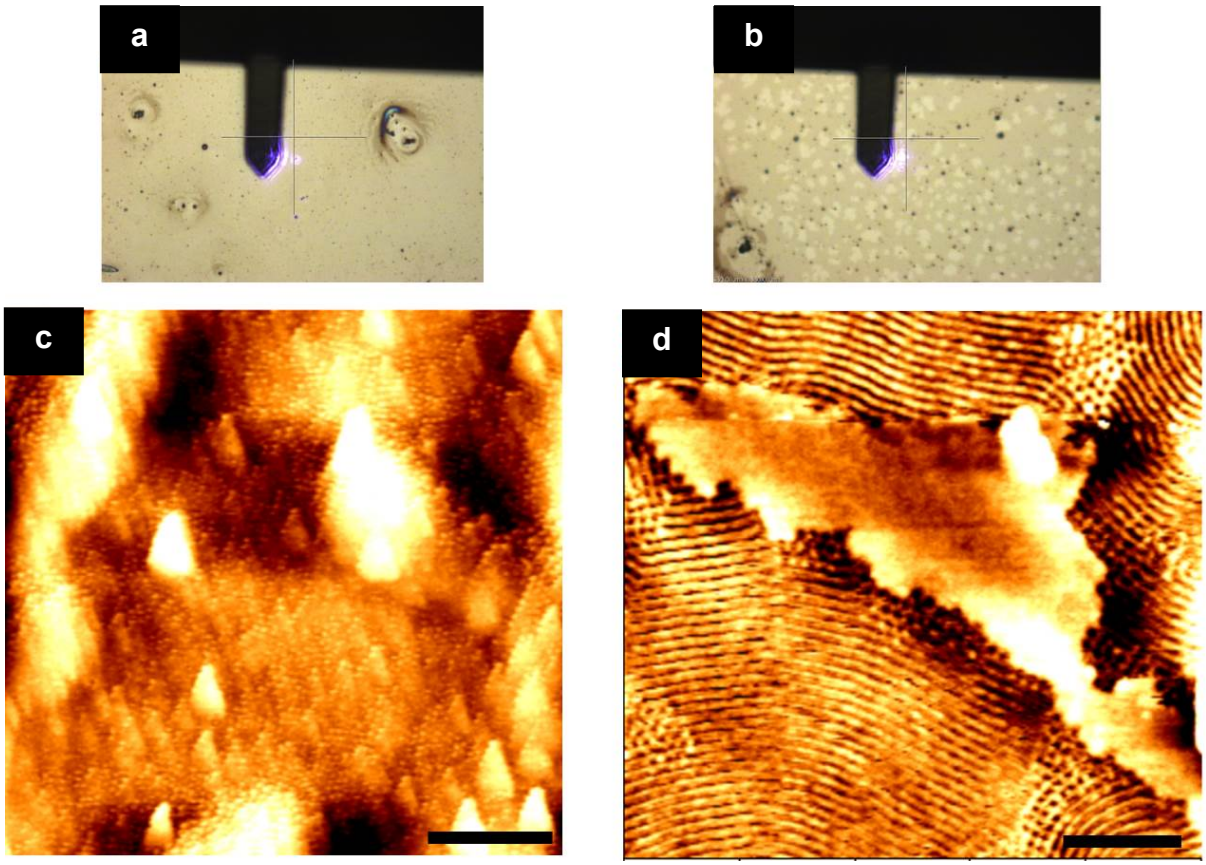

Figure S14. Optical images (~ 480 x 360 micron) of (a) as cast 0.5 wt % PS-*b*-P4VP on bare silicon sample without cleaning (contact angle, 37°) and (b) following 2 hours of solvent vapor annealing with chloroform. Corresponding AFM topographic images (scale bar = 400 nm) are shown in (c) and (d). (c) AFM topographic image of as cast film showing a poorly microphase separated pattern. (d) Following 2 hours solvent vapor annealing, the film shows well developed P4VP cylinders lying in plane. However a large defective area is seen in the AFM image. The non-uniform nature of the solvent vapor annealed film can be seen in the optical image in (b).

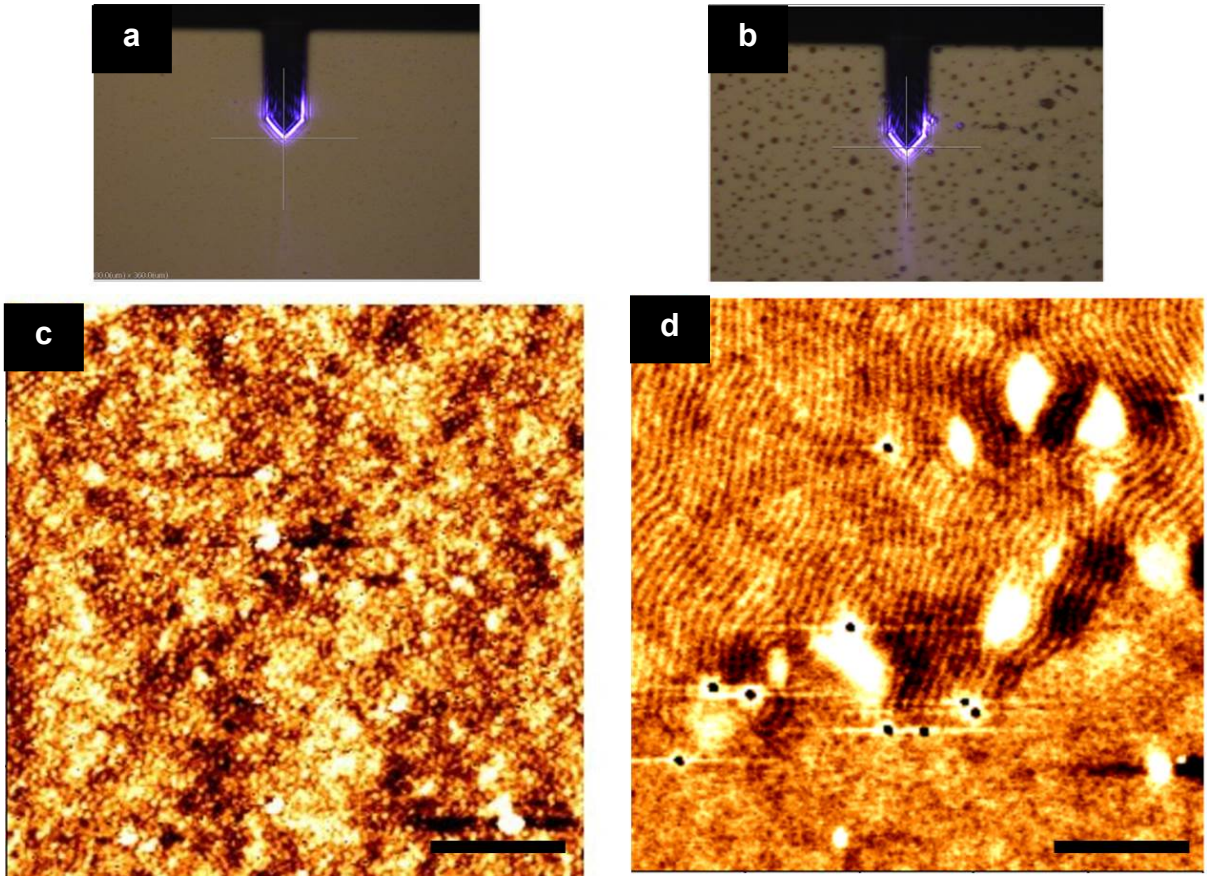

Figure S15. Optical images (~ 480 x 360 micron) of (a) as cast 0.5 wt % PS-*b*-P4VP on PS-OH functionalized silicon substrate (contact angle, 94°) and (b) following 2 hours of solvent vapor annealing with chloroform. Corresponding AFM topographic images (scale bar = 400 nm) are shown in (c) and (d). (c) AFM topographic image of as cast film showing P4VP cylinders normal to the silicon substrate. (d) Following 2 hours solvent vapor annealing, the film shows P4VP cylinders lying in plane. Dewetted areas as well as poorly microphase separated areas are also observed.

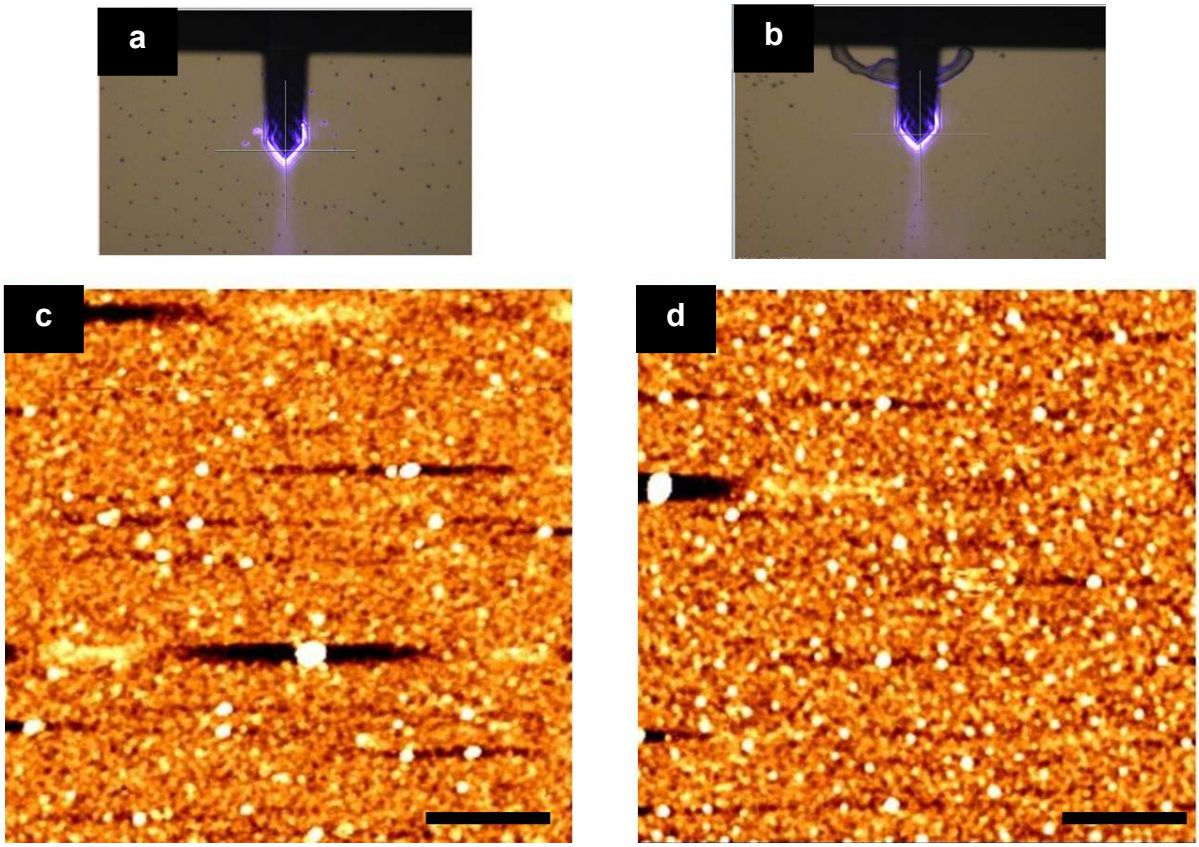

Figure S16. Optical images (~ 480 x 360 micron) of (a) as cast 0.5 wt % PS-*b*-P4VP BCP on PDMS-OH functionalized silicon substrate (contact angle, 104°) and (b) following 2 hours of solvent vapor annealing with chloroform. Corresponding AFM topographic images (scale bar = 400 nm) are shown in (c) and (d). Microphase separation was not observed in either sample, as seen from (c) as cast and (d) solvent vapor annealed.

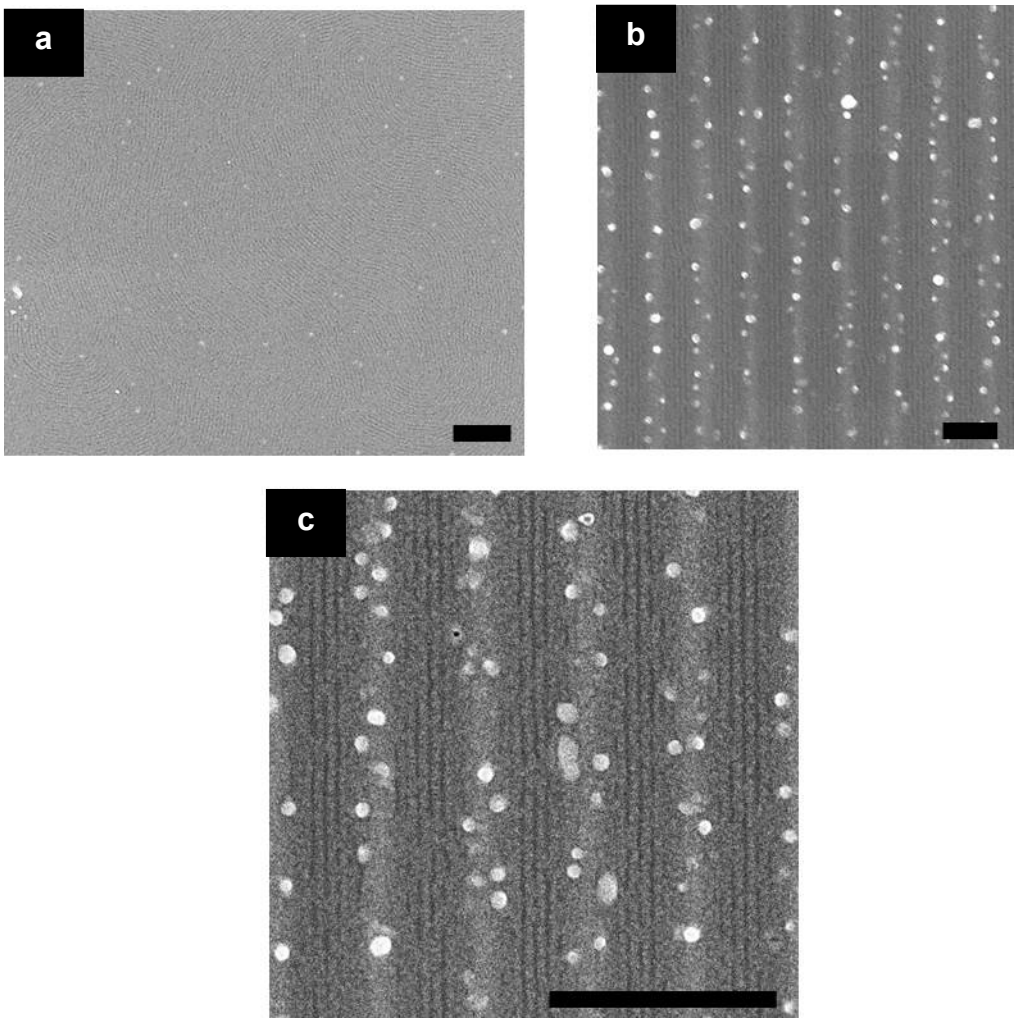

Figure S17. (a) Top-down SEM image of open area on HSQ patterned substrates showing P4VP cylinders lying in plane after self-assembly via solvent vapor annealing. (b) low resolution and (c) high resolution SEM images of P4VP cylinders lying in plane guided by 50 nm wide HSQ gratings at a channel width of 265 nm. Note that all images (a) – (c) were stained with ruthenium tetroxide for contrast purposes. All scale bars = 500 nm.

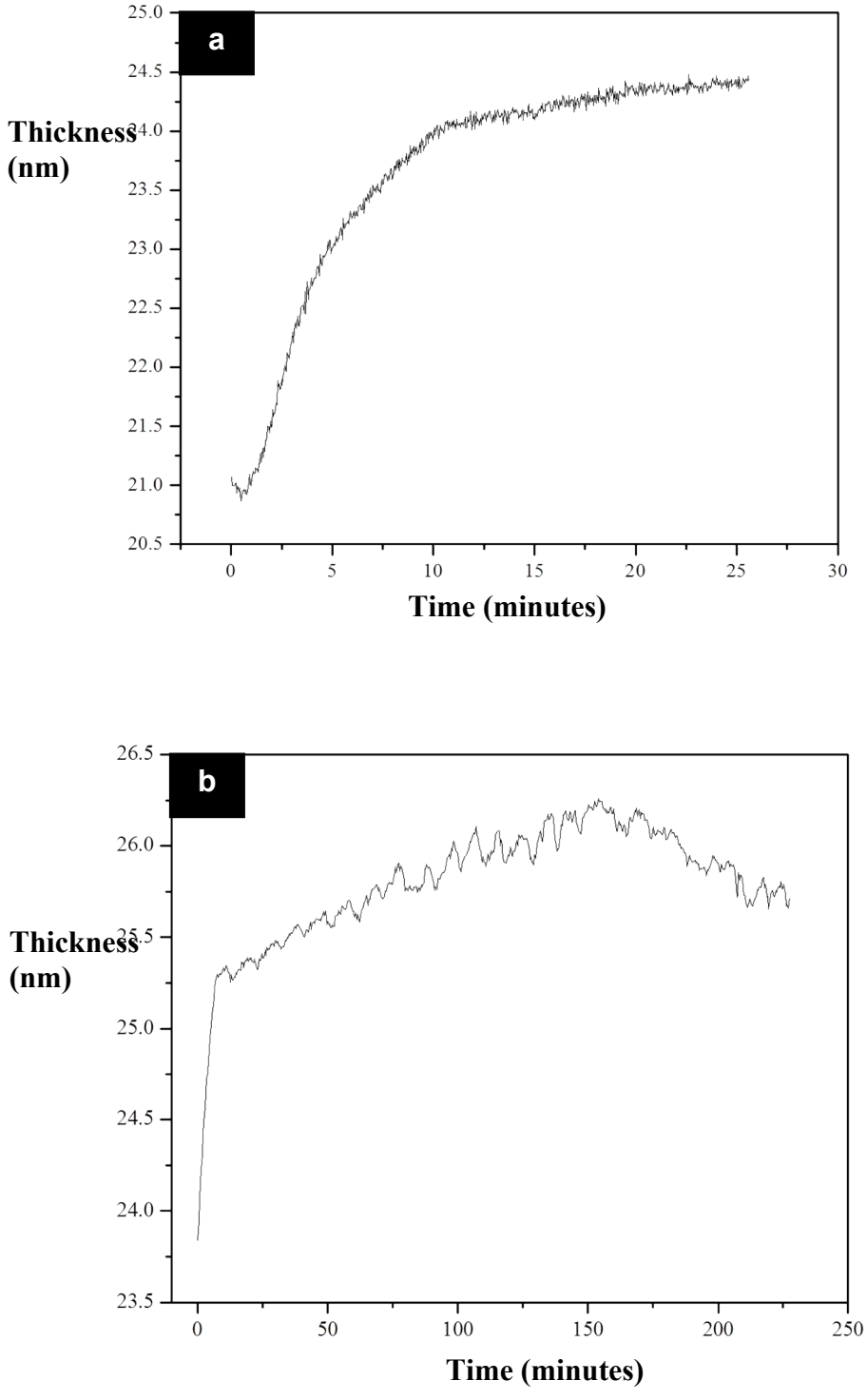

Figure S18. *In-situ* thickness measurement. Plot of thickness (nm) change versus time (minutes) of 0.5 wt % PS-*b*-P4VP BCP film spin coated on acetone only cleaned silicon followed by annealing with chloroform vapor for (a) 30 minutes and (b) 230 minutes. Both (a) and (b) indicate that the film does not rise more than 15% (~26.5 nm) from its initial thickness (~23nm).

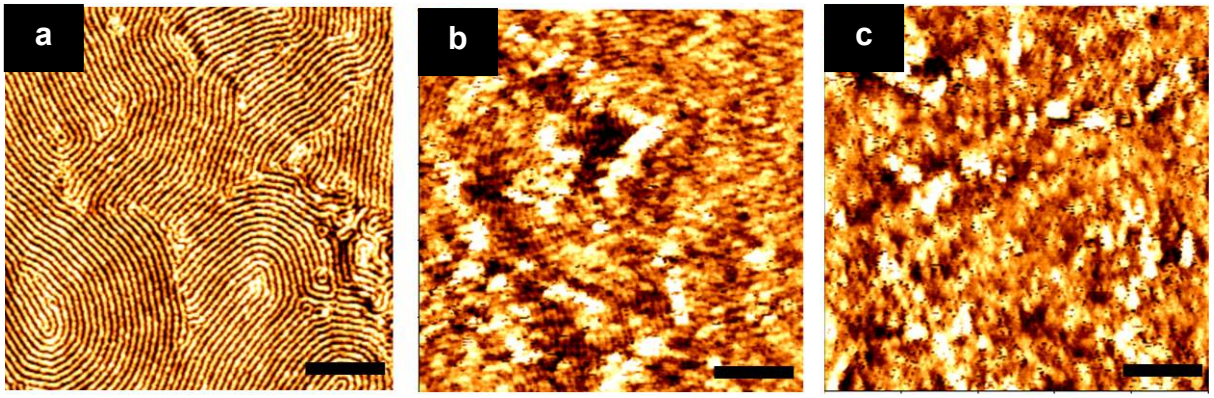

Figure S19. AFM topographic images (scale bars = 400 nm) of PS-*b*-P4VP BCP films following immersion in 10 ml ethanol for (a) 10 minutes, (b) 20 minutes and (c) 30 minutes. (b) and (c) show deformation of the original PS-*b*-P4VP BCP structure due to swelling of the P4VP nanodomains that distort the PS matrix.

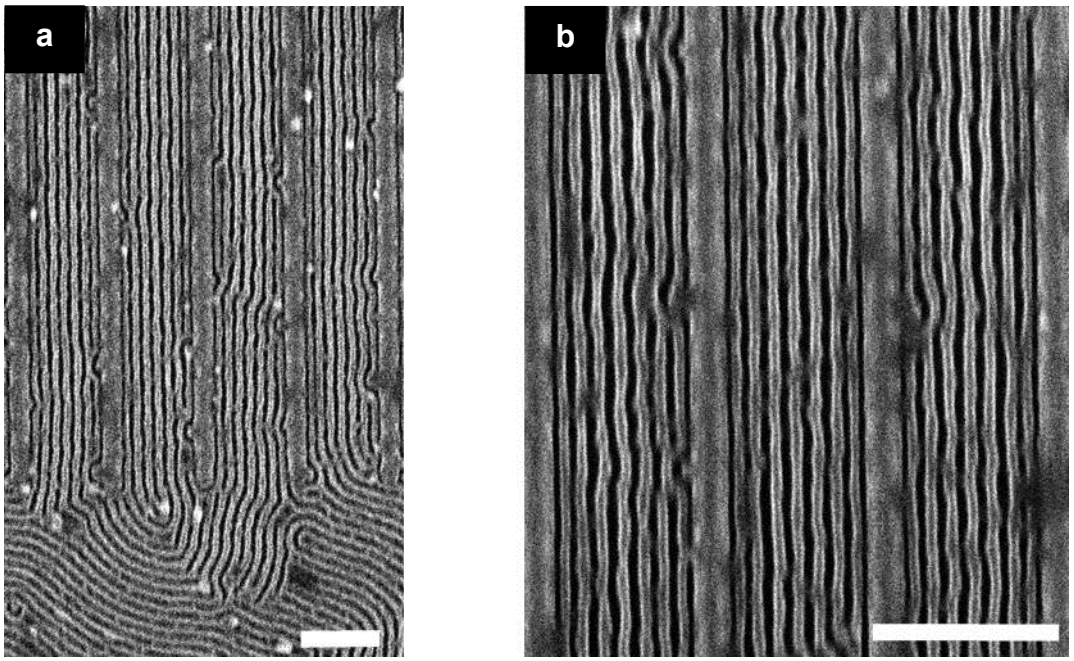

Figure S20. (a) and (b) show top-down SEM images of iron oxide nanowires where 50 nm wide HSQ prepatterns at a channel width of 265 nm that initially aligned PS-*b*-P4VP BCP material. Note that these samples were silicon etched for 5 seconds to improve contrast for SEM. Scale bars = 250 nm.

Figure S20a and b shows a top-down SEM image of the Fe_3O_4 nanowires with long range order. The periodicity of the nanowires and domain size distributions are similar to the original PS-*b*-P4VP self-assembled BCP template. Figure S20a shows an open area of the

substrate that exhibits the 'fingerprint' like pattern evidenced on planar substrates. As the pattern enters the trenches alignment takes place guided by the HSQ sidewalls. The alignment and registration of the Fe_3O_4 nanowires is shown for up to 2 microns in HSQ trenches with a channel width of 265 nm. A total of 7 Fe_3O_4 nanowire features can be seen in the SEM image. The high resolution SEM image in Figure S20b shows well-defined Fe_3O_4 nanowire patterns from a 265 nm trench.

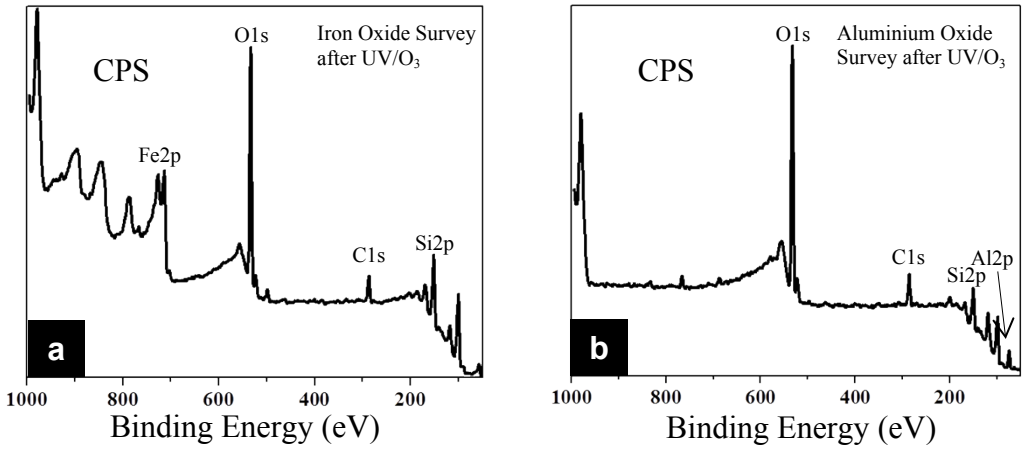

Figure S21. XPS survey spectrum of (a) Fe_3O_4 nanowires and (b) γ-Al_2O_3 nanowires formed via spin coating of metal nitrate-ethanolic solutions on porous PS-*b*-P4VP BCP followed by UV/O_3 for 3 hours.

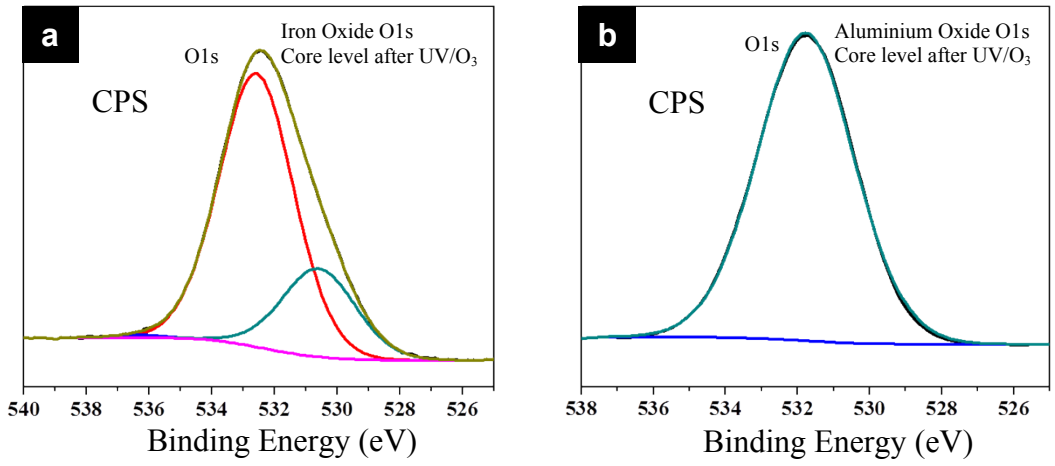

Figure S22. High resolution XPS spectra of O *1s* region from (a) Fe_3O_4 nanowires and (b) γ-Al_2O_3 nanowires.

Table of contents.